
Analysis of Ozone Mass Transfer in a Kenics Static Mixer Using the Steady State Back Flow Cell Model (BFCM)

*Mohamed. A. M. Saad *Abdullah. A. Elamari, *Awad.E. Alshebani

ABSTRACT: STATIC MIXERS HAVE BEEN SUCCESSFULLY EMPLOYED IN WATER AND WASTEWATER TREATMENT, PARTICULARLY IN WATER OZONATION FOR DISINFECTION AND OXIDATION PURPOSES. PRODUCING HIGHER CONCENTRATION OF OZONE REQUIRES NEW CONTACTORS THAT OPERATE EFFICIENTLY AT LOW GAS/LIQUID RATIO. THE KENICS STATIC MIXER CAN MEET THESE REQUIREMENTS AND THEREFORE ENHANCE THE OZONE MASS TRANSFER RATE [1]. THE FIRST OBJECTIVE OF THIS STUDY IS TO USE THE STEADY STATE BACK FLOW CELL MODEL (BFCM) DEVELOPED BY TIZAOU AND ZHANG [1] IN ORDER TO PREDICT THE OZONE CONCENTRATION PROFILE IN THE GAS AND THE LIQUID PHASES ALONG THE KENICS STATIC MIXER. THE SECOND OBJECTIVE IS TO DEVELOP A MATLAB CODE FOR THE BFCM OF THE STATIC MIXER. THE THIRD OBJECTIVE OF THE STEADY STATE BFCM IS TO STUDY THE IMPACT OF THE MAIN CHARACTERISTIC PARAMETERS: BACK FLOW RATIO (B) OF, THE LENGTH OF THE KENICS STATIC MIXER, FLOW RATE OF WATER (L), AND GAS FLOW RATE (G), VOLUMETRIC LIQUID MASS TRANSFER COEFFICIENT ($k_L a$) AND TEMPERATURE ON OZONE CONCENTRATION PROFILE IN THE GAS AND LIQUID PHASES (y/y_{in}) AND (x/x_{in}^*) RESPECTIVELY ALONG THE HEIGHT OF THE KENICS STATIC MIXER.

KEYWORDS: KENICS STATIC MIXER, BACK FLOW CELL MODEL, OZONE MASS TRANSFER.

1.0 INTRODUCTION

During the last few decades, new cheap ozone generators have been developed and they produce high ozone concentration, but they require low gas flow rates which result in low gas to liquid volumetric flow rate ratio. As a result, classical bubble columns are no longer applicable because they require a larger gas flow rate to achieve efficient mixing between gas and liquid and therefore high ozone mass transfer. However, Static mixers as shown in figure 1 are more efficient at low gas/liquid ratio and high concentration of ozone and therefore they provide a solution to this problem. Moreover, static mixers produce a homogeneous ozone concentration because of the high turbulence produced by the elements that are inside the mixer, which ensure adequate gas/liquid mixing [2,1].

* Chemical Engineering Department, Sirte University, Sirte, Libya

* Chemical Engineering Department, Sirte University, Sirte, Libya

* Chemical Engineering Department, Sirte University, Sirte, Libya

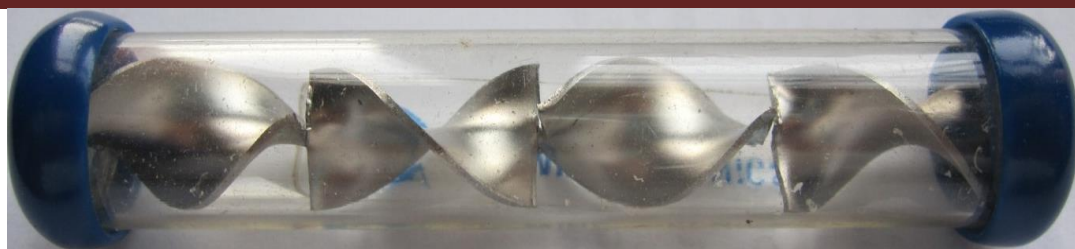


Figure 1: Kenics static mixer (source: Chemineer Inc.)

2. THE STEADY STATE BACK FLOW CELL MODEL (BFCM) FOR OZONE MASS TRANSFER IN THE STATIC MIXER

The BFCM of Tizaoui and Zhang [1] has been built to predict the ozone concentration profile in a Kenics static mixer. In BFCM model, both back flow and exchange have been hypothesized to describe the axial dispersion in the liquid phase. Figure 2 below shows a schematic representation of BFCM for upward co-current flow conditions in the static mixer. In order to study the effect of backmixing in the liquid phase, a fraction (B) of the inlet liquid flow to each cell returned back from the upper stage to the lower adjacent stage and this referred to as back flow. At the same time, exactly the same portion of the liquid flow is transferred from the lower stage to the closet upper stage and this process is referred to as exchange flow. Both back flow (B) and exchange flow ratios have been assumed to be equal and also constant along the length of the mixer. BFCM model is comprised of two series of number (N) of completely mixed cells. One of these two series represents the liquid phase and the other one represents the gas phase and both phases have equal number of cells (N). The first and the last cells (0 and N+1) in the figure 2 represent virtual cells with negligible volume and hold-up. Therefore, the exchange flow rate (backmixing) at the boundary of the static mixer can be easily determined. Back mixing is characterised by two parameters: number of stages and the Peclet number.

Several assumptions have been used in the developing the steady state BFCM: (1) the system is operated at steady-state and isothermal conditions; (2) Henry's law applies for ozone equilibrium concentration in water; (3) the mass transfer coefficient (k_L) are constant throughout the mixer height; (4) dilute system; (5) the ozone decay rate is described by pseudo-first order in the liquid phase but it is negligible in gas phase; (6) back flow takes place only in the liquid phase; (7) back flow in the gas phase is negligible because of the large

buoyancy of gas bubble; (8) gas and liquid flow rate are constant throughout the mixer height; (9) interfacial area and gas hold-up are constant along the mixer height; (10) the resistance to the ozone mass transfer is confined to the liquid bulk only.

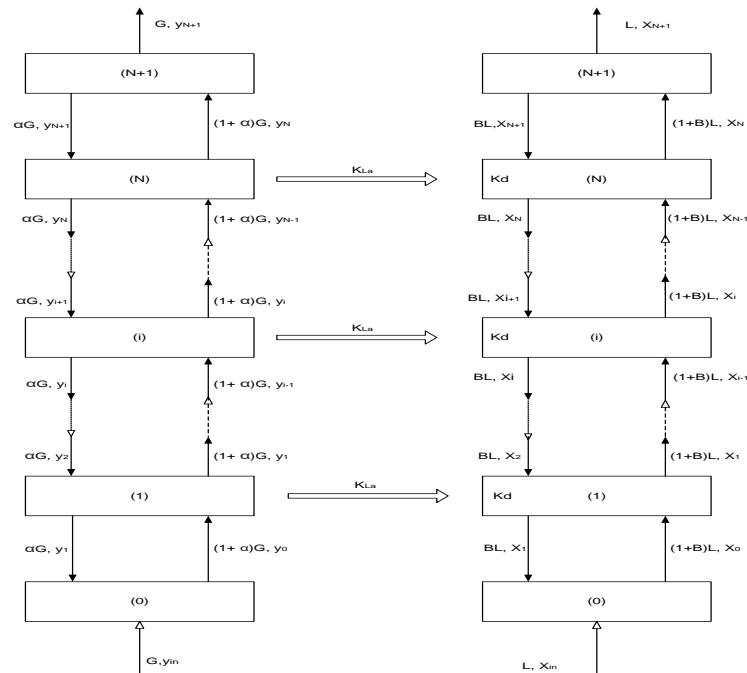


Figure 2: Schematic representation of the steady state BFCM

(G : molar gas flow rate (mol/s); L : molar liquid flow rate (mol/s); x : mole fraction of ozone in the liquid phase; y : mole fraction of ozone in the gas phase; i : cell number; N : total number of cells; B : back flow ratio in the liquid phase; α : back flow ratio in the gas phase; k_d : pseudo first order ozone decay rate constant (s^{-1}))

It is assumed that the mass transfer occurs at the interface between the adjacent cells. The ozone mass transfer rate (Ψ) can be estimated according to the two-film theory model:

$$\Psi = k_L a (x_L^* - x_L) \quad (1)$$

Where: Ψ is the ozone mass transfer rate per unit volume, k_L is local liquid mass transfer coefficient, a is specific interfacial area, x_L^* is the concentration of dissolved gas in equilibrium with bulk gas and x_L is the concentration of the dissolved gas in the bulk liquid.

The gaseous ozone travels much faster through the gas phase rather than the liquid phase. Therefore, ozone mass transfer rate in the liquid phase becomes controlling parameter and the total mass transfer can be described by the liquid mass transfer coefficient $k_L a$. The $k_L a$ value used in this study is $0.1 s^{-1}$ [3].

The equilibrium liquid concentration of ozone x_i^* can be calculated by the following formula:

$$x_i^* = \frac{y_i}{m} \quad (2)$$

$$m = \frac{H}{P_T} \quad (3)$$

Where: P_T is the total pressure drop across the static mixer and H is the Henry's constant and it is estimated by the following formula [4]:

$$H = 3.84 \times 10^7 (10^{pH-14})^{0.035} \exp\left(-\frac{2428}{T}\right) \quad (4)$$

Hoigne (1982) (cited in Gamal El-Din and Smith [5]) mentioned that as gaseous ozone dissolves in the liquid water and due to its very high oxidative nature, it begins to decay by auto-decomposition and oxidation of pollutant present in water. The ozone decay rate or the ozone chemical reaction rate depends on water temperature, pH and water content and it can be described by the following correlation [6]:

$$R = Ek_d C_i \quad (5)$$

$$k_d = 5.43 \times 10^3 \exp\left(-\frac{4964}{T}\right) \quad (6)$$

Where k_d is the pseudo first order auto decomposition rate constant in (s^{-1}), where its value is equal to $2.4030e-004s^{-1}$ and the T is the temperature in K [1,5].

Since ozone is sparingly soluble in water, the chemical reaction of ozone is slow and consequently the enhancement factor of the chemical reaction to the ozone mass transfer coefficient is equal to 1.0. Slow chemical reactions reduce the concentration of the gaseous ozone in the water bulk resulting in higher driving force for mass transfer. Moreover, increasing the reaction rate will lead to a higher mass transfer coefficient. Thus, Hatta number is used to account for the contribution of the chemical reaction to the mass transfer process:

$$Ha^2 = \frac{D_{O_3} k_d}{k_L^2} \quad (7)$$

The value of the ozone diffusivity coefficient D_{O_3} is equal to $1.76 \times 10^{-9} \text{ m}^2/\text{s}$ [2].

From equation 7, it was found that the value of the Hatta number, $Ha = 6.5033e-006$. Therefore, it has been concluded that the chemical reaction of the ozone with the pollutants present in the water has a negligible effect on the liquid side mass transfer coefficient. The Kenics static mixer consists of 39 cells with length of 0.74m and internal diameter of 0.0191m. The liquid and gas flow rates are 0.03 and 0.0067L/s respectively [1].

For upward and co-current mode shown in Figure 2, the basic mass balance for the ozone dissolved in the gas phase in each cell is:

For $i = 0$:

$$Gy_{in} + \alpha Gy_1 - (1 + \alpha)Gy_0 = 0 \quad (8)$$

For $1 \leq i \leq N$:

$$(1 + \alpha)Gy_{i-1} + \alpha Gy_{i+1} - \alpha Gy_i - (1 + \alpha)Gy_i - k_1 av_c (x_i^* - x_i) = 0 \quad (9)$$

For $i = N+1$:

$$(1 + \alpha)Gy_N - \alpha Gy_{N+1} - Gy_{N+1} = 0 \quad (10)$$

Now, the mass balance of the dissolved ozone in the liquid phase:

$$\text{For } i = 0: \quad Lx_{in} + BLx_1 - (1 + B)Lx_0 = 0 \quad (11)$$

For $i = 1$:

$$(1 + B)Lx_0 + BLx_2 - (1 + B)Lx_1 - BLx_1 + k_1 av_c (x_1^* - x_1) - k_d x_1 = 0 \quad (12)$$

For $2 \leq i \leq N$:

$$(1 + B)Lx_{i-1} + BLx_{i+1} - (1 + B)Lx_i - BLx_i + k_1 av_c (x_i^* - x_i) - k_d x_i = 0 \quad (13)$$

$$\text{For } i = N: \quad (1 + B)Lx_N - BLx_{N+1} - Lx_{N+1} = 0 \quad (14)$$

3. THE NUMERICAL SOLUTION OF THE STEADY STATE BFCM MODEL

Mass balance equations for the gas phase:

It is assumed that the backmixing in the gas phase (α) is negligible and also the gas flow rate is constant along the static mixer. Therefore, equation 1 can be written as:

$$\text{For } i = 0$$

$$\alpha = 0 \Rightarrow Gy_{in} - Gy_0 = 0 \Rightarrow Gy_{in} = Gy_0$$

$$y_{in} = y_0 \quad (15)$$

$$\text{For } 1 \leq i \leq N$$

$$\alpha = 0 \Rightarrow Gy_{i-1} - Gy_i - k_L aV(x_i^* - x_i) = 0$$

$$y_{i-1} - y_i - (k_L aV/G)(x_i^* - x_i) = 0$$

$$a_4 = \frac{k_L aV}{G} \Rightarrow y_{i-1} - y_i - a_4(x_i^* - x_i) = 0$$

$$y_{i-1} - y_i + a_4 x_i - a_4 x_i^* = 0 \quad (16)$$

$$\text{For } i = N + 1$$

$$\alpha = 0 \Rightarrow Gy_N - Gy_{N+1} = 0$$

$$y_{N+1} = y_{out} = y_N \quad (17)$$

Mass balance around the liquid phase

It is assumed that the gas flow rate is constant along the static mixer. Therefore, equations can be written as:

$$\text{For } i = 0$$

$$a_0 = (1 + B) \text{ and } a_2 = B \Rightarrow x_{in} + a_2 x_1 - a_0 x_0 = 0 \quad (18)$$

$$\text{For } i = 1$$

$$a_3 = k_L aV/L \text{ and } a_1 = (1 + 2B + k_L aV/L + k_d/L) \Rightarrow a_0 x_0 - a_1 x_1 + a_2 x_2 + a_3 x_1^* = 0$$

$$\text{from equation (11), we have } a_0 x_0 = a_2 x_1 - x_{in} \Rightarrow (a_2 - a_1)x_1 + a_2 x_2 + a_3 x_1^* = x_{in} \quad (19)$$

$$\text{For } 2 \leq i \leq N$$

$$a_0 = (1 + B) \text{ and } a_1 = (1 + 2B + k_L aV/L + k_d/L), a_2 = B, a_3 = \frac{k_L aV}{L} \\ \Rightarrow a_0 x_{i-1} - a_1 x_i + a_2 x_{i+1} + a_3 x_i^* = 0 \quad (20)$$

$$\text{For } i = N + 1$$

$$(1 + B)Lx_N - (1 + B)Lx_{N+1} = 0 \Rightarrow x_N = x_{out} = x_{N+1} \quad (21)$$

The next step is to convert the mass balance equations into a matrix form
For the gas phase

$$\text{For } 1 \leq i \leq N, \quad y_{i-1} - y_i + a_4 x_i - a_4 x_i^* = 0$$

$$\text{For } i = 1, \quad y_0 - y_1 + a_4 x_1 - a_4 x_1^* = 0$$

From equation 15, we have $y_0 = y_{in}$

$$i = 1, \quad -y_1 + a_4 x_1 - a_4 x_1^* = -y_{in}$$

$$i = 2, \quad y_1 - y_2 + a_4 x_2 - a_4 x_2^* = 0$$

$$i = 3, \quad y_2 - y_3 + a_4 x_3 - a_4 x_3^* = 0$$

$$i = N, \quad y_{N-1} - y_N + a_4 x_N - a_4 x_N^* = 0$$

The above equations have been converted to the following matrix:

$$\begin{bmatrix} -y_1 & 0 & 0 & 0 & \dots & 0 \\ y_1 & -y_2 & 0 & 0 & \dots & 0 \\ 0 & y_2 & y_3 & 0 & \dots & 0 \\ 0 & 0 & y_3 & -y_4 & \dots & 0 \\ \vdots & \vdots & \vdots & \vdots & \ddots & \vdots \\ 0 & 0 & 0 & 0 & y_{N-1} & -y_N \end{bmatrix}$$

From the concept that $Ay=B$ [7, 8], the above matrix can be written as $[GM]\bar{y} = [\overline{GB}]$

Where:

$$\bar{y} = \begin{bmatrix} y_1 \\ y_2 \\ y_3 \\ y_4 \\ \vdots \\ y_N \end{bmatrix} [GM] = \begin{bmatrix} -1 & 0 & 0 & 0 & \dots & 0 \\ 1 & -1 & 0 & 0 & \dots & 0 \\ 0 & 1 & -1 & 0 & \dots & 0 \\ 0 & 0 & 1 & -1 & \dots & 0 \\ \vdots & \vdots & \vdots & \vdots & \ddots & \vdots \\ 0 & 0 & 0 & 0 & 1 & -1 \end{bmatrix} \overline{GB} = \begin{bmatrix} -y_{in} \\ 0 \\ 0 \\ 0 \\ \vdots \\ 0 \end{bmatrix}$$

For the liquid phase

$$i = 1, \quad (a_2 - a_1)x_1 + a_2 x_2 + a_3 x_1^* = x_{in}$$

$$\text{For } 2 \leq i \leq N, \quad a_0 x_{i-1} - a_1 x_i + a_2 x_{i+1} + a_3 x_i^* = 0$$

$$i = 2, \quad a_0 x_1 - a_1 x_2 + a_2 x_3 + a_3 x_2^* = 0$$

$$i = 3, \quad a_0 x_2 - a_1 x_3 + a_2 x_4 + a_3 x_3^* = 0$$

$$\text{For } i = N, \quad a_0 x_{N-1} - a_1 x_N + a_2 x_{N+1} + a_3 x_N^* = 0$$

From equation (14), we have $x_N = x_{N+1} \Rightarrow$

$$i = N, \quad a_0 x_{N-1} + (a_2 - a_1)x_N + a_3 x_N^* = 0$$

From the correlation, $Ax=B$, the above equations can be written as $[LM]\bar{x} = [\overline{LB}]$

Where:

$$\bar{x} = \begin{bmatrix} x_1 \\ x_2 \\ x_3 \\ x_4 \\ \vdots \\ x_N \end{bmatrix} [LM] = \begin{bmatrix} (a_2 - a_1) & a_2 & 0 & 0 & 0 & 0 & \dots & 0 \\ a_0 & -a_1 & a_2 & 0 & 0 & 0 & \dots & 0 \\ 0 & a_0 & a_1 & a_2 & 0 & 0 & \dots & 0 \\ 0 & 0 & a_0 & -a_1 & a_2 & 0 & \dots & 0 \\ 0 & 0 & 0 & a_0 & -a_1 & a_2 & \dots & 0 \\ 0 & 0 & 0 & 0 & a_0 & -a_1 & \dots & 0 \\ \vdots & \vdots & \vdots & \vdots & \vdots & \vdots & \ddots & 0 \\ 0 & 0 & 0 & 0 & 0 & 0 & a_0 & (a_2 - a_1) \end{bmatrix} [LB]$$

$$= \begin{bmatrix} x_{in} \\ 0 \\ 0 \\ 0 \\ 0 \\ \vdots \\ 0 \end{bmatrix}$$

All the previous steps can be summarised in the following three equations:

$$[LM]\bar{x} + a_3\bar{x}^* = \bar{LB} \quad (22)$$

$$[GM]\bar{y} + a_4\bar{x} - a_4\bar{x}^* = \bar{GB} \quad (23)$$

$$\bar{x}^* = \frac{1}{m}\bar{y} \quad (24)$$

By substituting equation (24) into equation (22), the following equation is produced:

$$\bar{x} = [LM]^{-1}\bar{LB} - \frac{a_3}{m}[LM]^{-1}\bar{y} \quad (25)$$

And then substitute equation (25) into equation (22), we will have:

$$\bar{y} \left([GM] - \frac{a_3 a_4}{m} [LM]^{-1} - \frac{a_4}{m} \right) = \bar{GB} - a_4 [LM]^{-1} \bar{LB}$$

For simplification purposes, it has been assumed that:

$$[A] = [GM] - \frac{a_3 a_4}{m} [LM]^{-1} - \frac{a_4}{m} \quad (26)$$

$$\bar{C} = \bar{GB} - a_4 [LM]^{-1} \bar{LB} \quad (27)$$

As a result of these assumptions, the following equation is produced:

$$\begin{aligned} \bar{y}[A] &= \bar{C} \Rightarrow \bar{y} \\ &= [A]^{-1}\bar{C} \end{aligned} \quad (28)$$

Substituting equation (28) into equation (25) result in:

$$\bar{x} = [LM]^{-1}LB - \frac{a_3}{m} [LM]^{-1}[A]^{-1}\bar{C} \quad (29)$$

Substituting equation 28 into equation 2 result in:

$$\bar{x}^* = \frac{1}{m} [A]^{-1}\bar{C} \quad (30)$$

The equations: 2, 3, 6, 7, 26, 27, 28, 29 and 30 and the constants: a_0, a_1, a_2, a_3, a_4 have been implemented in a Matlab software in order to estimate the ozone concentration in the gas and liquid phases and also to study the impact of the design parameters on the ozone mass transfer rate as shown in Appendix I and II respectively.

4.0 RESULTS AND DISCUSSION

4.1 THE CONCENTRATION PROFILE ALONG THE HEIGHT OF THE STATIC MIXER

Figure 3: presents the liquid and gas concentration profile of the ozone along the height of the Kenics static mixer. The characteristics of the Modelled static mixer are: 39 cells inserted in line through the length of the mixer, total length of 0.74m, internal diameter of 0.0191m and it operates at gas to liquid volumetric ratio of 0.22. The gas and liquid flow rates and inlet ozone concentration values are 0.41L/min, 1.8L/min and 64g/m^3 respectively.

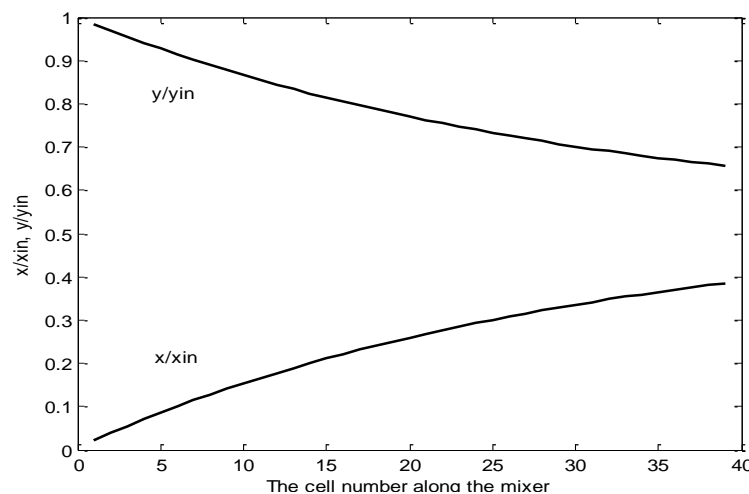


Figure 3: The ozone concentration in the gas and liquid phase along the height of the static mixer ($N=39$, $L=0.03\text{L/s}$, $G=0.0067\text{L/s}$, $y_{in}=0.064\text{g/L}$, $\text{Length}=0.74$, $T=20\text{C}$, $B=0.33$, $k_L a = 0.1\text{s}^{-1}$)

From the graph, it can be clearly seen, and as was expected that the ozone concentration in the gas phase (y/y_{in}) decreases across the height of the static mixer. On the other hand, the ozone concentration in the liquid phase (x/x_{in}^*) increases as the liquid passes along the height of the static mixer. This trend in the ozone concentration profile can be explained by the fact

that the main purpose of the water ozonation process inside the Kenics static mixer is to transfer the ozone from the gas phase to the liquid phase so the ozone can react with pollutants present in the water. The exit ozone concentration in the gas phase and the liquid phase are still far from the equilibrium state which can be defined as the state at which the ozone gas concentration (y/y_{in}) is equal to the ozone liquid concentration (x/x_{in}^*). This non-equilibrium state ($y/y_{in} \neq x/x_{in}^*$) is due to the short contact time between the gas phase and the liquid phase inside the static mixer [1].

There is a slightly more rapid decrease in the ozone gas concentration and also more rapid increase in the ozone liquid concentration at the bottom of the Kenics static mixer. This may be because of the higher degree of turbulence and higher shear rates at the entrance of the mixer which results in smaller bubbles and therefore larger gas-liquid interfacial area and subsequently higher mass transfer rate of ozone from the gas phase to the liquid phase [9].

4.2 THE EFFECT OF THE VOLUMETRIC MASS TRANSFER COEFFICIENT ($K_L A$) ON THE OZONE MASS TRANSFER

The volumetric liquid mass transfer coefficient is key parameter to describe the rate of ozone mass transfer in a Kenics static mixer. It is the product of the interfacial area (a) and liquid mass transfer coefficient (k_L). The impact of physical variables such as density, surface tension and viscosity and the process variables such as flow rates of gas and liquid and the mixer shape and dimension can be represented by the $k_L a$ [1]. Since the Ozone gas is slightly soluble in water, the resistance to ozone mass transfer in the gas phase is assumed to be negligible. Consequently, the liquid film is the controlling factor for the ozone mass transfer rate. In this model, the rate of ozone mass transfer in the Kenics static mixer was estimated by the following kinetic correlation (eq.1):

$$\Psi = K_L a V \Delta C$$

The model was run to simulate the change in the gas and the liquid concentration profile along the column as a function of the volumetric mass transfer coefficient ($K_L a$) so that the

approach to equilibrium can be studied. As shown in figure 4, and as the K_{La} increased from $0.09s^{-1}$ to $0.2s^{-1}$, a continuous increase in the dissolved ozone concentration in the liquid phase occurred along the mixer whereas continuous reduction in the dissolved ozone concentration in the gas phase occurred along the mixer and also at the outlet of the static mixer. For all values of K_{La} and especially at the highest value of $0.2s^{-1}$, most of the gaseous ozone was consumed before reaching the top of the mixer height and this leads to a lower driving force for the mass transfer process and therefore results in a smaller amount of ozone residual in the effluent stream. At larger K_{La} values, the increasing and the decreasing trends in the ozone concentration profile in the liquid and gas phase respectively were faster than those at low K_{La} . This is due to the high value of the mass transfer rates that cause faster depletion of the ozone in the gas phase and faster transportation of ozone to the liquid phase. It is very noticeable from the graph that the liquid ozone concentration (x/x_{in}^*) at $K_{La} = 0.2s^{-1}$ has dramatically increased from around 0.06 at the first cell to about 0.5 at cell number 25 and after that it slightly and steadily increased along the rest of the mixer height.

However, at $K_{La} = 0.09s^{-1}$, the ozone liquid concentration has monotonically increased along the height of the mixer. Based on these observations, it has been concluded that a smaller number of cells are required for the high values of K_{La} .

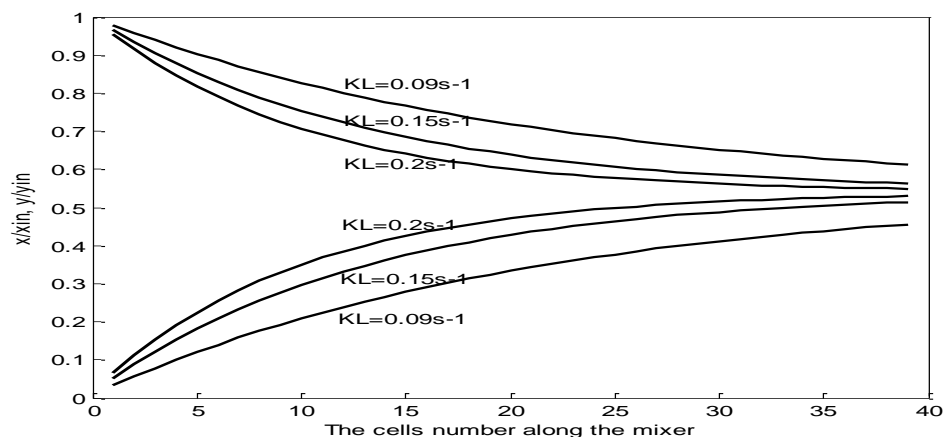


Figure 4: The effect of the volumetric mass transfer coefficient ($k_L a$) on the performance of the Kenics static mixer

4.3 THE EFFECT OF THE LENGTH OF THE KENICS STATIC MIXER (L) ON THE OZONE MASS TRANSFER

Figure 5 illustrates the impact of the length of the Kenics static mixer on the gas and liquid concentration profile of the ozone along the height of the static mixer. The performance of the mixer has been tested at three different lengths: 0.74, 2, 2.8 m. As it can be seen from the figure 5, and as the length of the mixer increases, there has been a continuous decrease and increase in the gas and liquid concentration of the ozone respectively along the height of the mixer and also at the outlet of the contactor. The static mixer of 2.8 m length has provided the best performance in terms of approaching the equilibrium between the gas and liquid ozone concentration. In theory, the equilibrium state between gas and liquid can only be reached by using a static mixer of an infinite length [1]. A static mixer of 2 m length has achieved relatively similar results to the 2.8 m length static mixer and therefore it can be considered as the optimum choice because the gas and liquid concentrations of the ozone are closer to equilibrium than the 0.74 m length mixer and at the same time it has less capital cost than the 2.8 m length mixer.

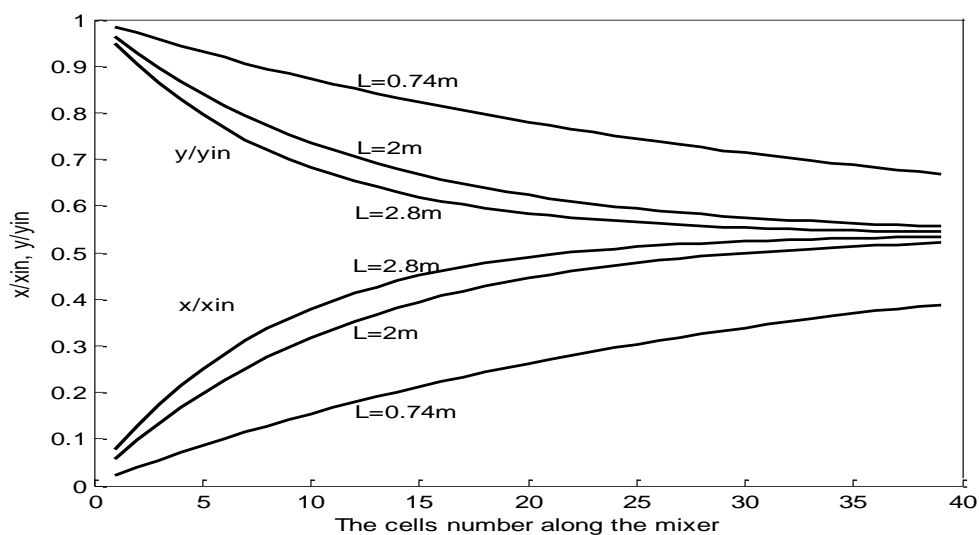


Figure 5: The effect of the height on the performance of the static mixer

4.4 THE EFFECT OF THE GAS AND LIQUID FLOW RATES (G AND L) ON THE OZONE MASS TRANSFER

Figures 6 and 7 depict the effect of gas and liquid flow rates on the gas and liquid concentration profile of the ozone. In figure 6, and as the gas flow rate was increased from 0.0033L/s to 0.0167L/s at a given liquid flow rate, the exit ozone liquid concentration (x/x_{in}^*) increased from around 0.3 to 0.7 and the exit ozone gas

concentration (y/y_{in}) decreased from about 0.8 to 0.4. On the other hand, as shown in figure 7, increasing the liquid velocity from 0.005L/s to 0.0667L/s results in a decrease in the liquid concentration (x/x_{in}^*) from 0.87 to 0.25 and also the gas concentration has dropped from 0.9 to 0.3.

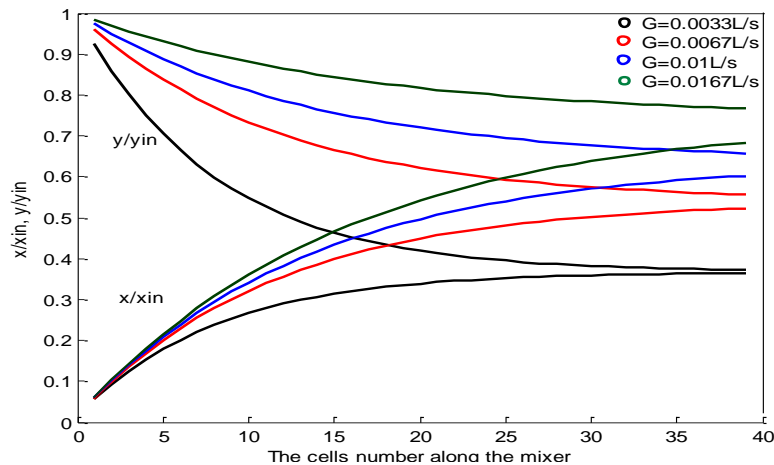


Figure 6: Effect of the gas velocity on the ozone concentration profile

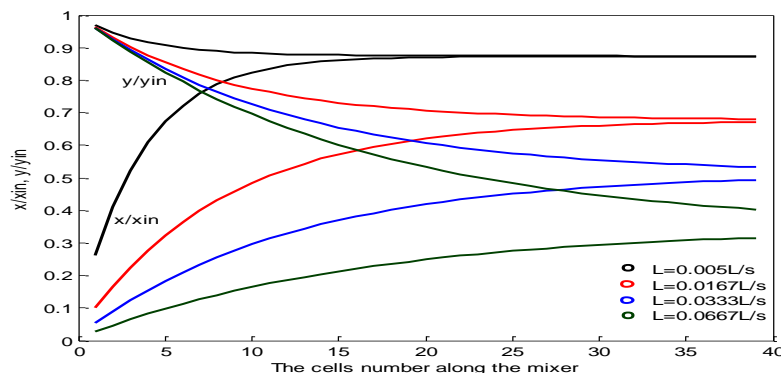


Figure 7: The effect of liquid velocity on the ozone concentration profile

Based on these observations, it can be said that increasing the gas flow rate resulted in an increase in the rate of mass transfer of ozone from the gas phase to the liquid phase whereas increasing the liquid flow rate leads to a reduction in the rate of ozone mass transfer. This can be ascribed to the fact that increasing the gas velocity will lead to a smaller gas-liquid interfacial area and therefore higher volumetric mass transfer coefficient, but increasing the liquid velocity results in a larger interfacial area.

These results agree with the findings of Sanchez et al., [10] and also with the findings of Heyouni et al., [3]. They stated that the higher the value of the gas velocity, the larger

the diameter of the gas bubbles. However, the bubble diameter decreases as the liquid velocity increase. This has been ascribed to the fact that higher energy input is required for high liquid velocities. This high power results in higher turbulence which causes the large bubbles to break into smaller bubbles. Thus, it results in higher ozone mass transfer efficiency. However, when Heyouni et al., [3] studied the effect of gas and liquid velocities on the interfacial area (a) and the mass transfer coefficient ($k_L a$), It was found that the ($k_L a$) and (a) increase with increasing either the gas or liquid velocities.

Gamal El-Din and Smith [11] have mentioned that the back flow ratio increases with increasing the gas flow rate. This can be explained by the fact that as the gas flow rate increases, the sizes of the bubbles increase with increasing the gas flow rate leading to a higher degree of circulation inside the mixer and therefore high backmixing. On the other hand, the back flow ratio decreases as the liquid flow rate increases. This is because the liquid flow approaches the plug flow regime at higher liquid flow rates.

Ozone transfer efficiency is a key design parameter due to the fact that most of the energy used in the water ozonation process is consumed in the ozone generation stage. Therefore, the loss of ozone in the off-gas can cause the process to be uneconomical [1].

$$\text{Ozone transfer efficiency} = \frac{Y_{i,N} - Y_{yi,0}}{Y_{i,N}} \times 100 \quad (31)$$

As shown in figure 8, as the liquid velocities increased from 0.001 to 0.05L/s, the ozone transfer efficiency increased from 10 to 93%. However, increasing the liquid flow rate to values above 0.05L/s resulted in very little improvement in the ozone transfer efficiency. The ozone transfer efficiency reaches maximum values at the highest liquid flow rates but with low G/L ratio. These results confirm the findings of the experiment of Craik et al., [12], where it was found that the maximum ozone mass transfer efficiency was obtained at high liquid velocity and low gas/liquid superficial velocity. These results prove the fact that the static mixers achieve the high ozone mass rates at low gas flow rate and low gas to liquid flow ratio (G/L).

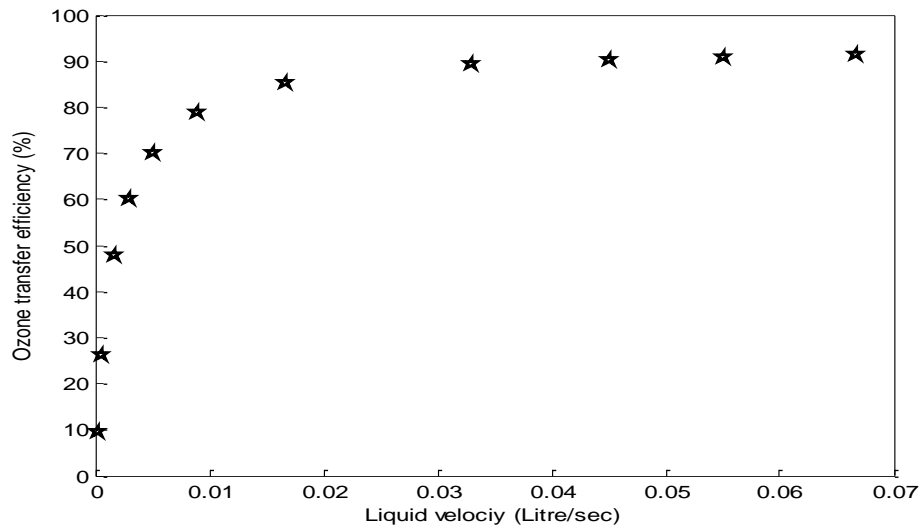


Figure 8: The relation between the liquid velocity and the ozone mass transfer efficiency of the mixer

4.5 THE EFFECT OF THE TEMPERATURE ON THE OZONE MASS TRANSFER

The effect of the temperature on the gas and liquid concentration at the outlet of the mixer was studied and the results are shown in figure 9. The figure shows that the exit gas concentration (y/y_{in}) is more sensitive to changes in temperature than the liquid concentration (x/x_{in}^*).

Figure 9 shows that as the temperature increases, the ozone liquid concentration at the outlet of the mixer increases while the exit gas concentration decreases. These observations can be compared to the theoretical understanding of the ozone reactions in the liquid phase. The slow chemical reaction occurs in the liquid bulk (water) after gas (ozone) absorption and it causes a reduction in the ozone concentration in liquid bulk and its rate is described by the following correlations (eq.5 and eq.6):

$$R = k_d C_i$$

$$k_d = 5.43 \times 10^3 \exp\left(-\frac{4964}{T}\right)$$

The temperature is inversely proportional to the first order rate constant of ozone decay (k_d) in water. Thus, high temperatures will result in smaller values of k_d and subsequently lower reaction rate and therefore the ozone concentration in the liquid phase will be larger than those concentrations at lower temperatures.

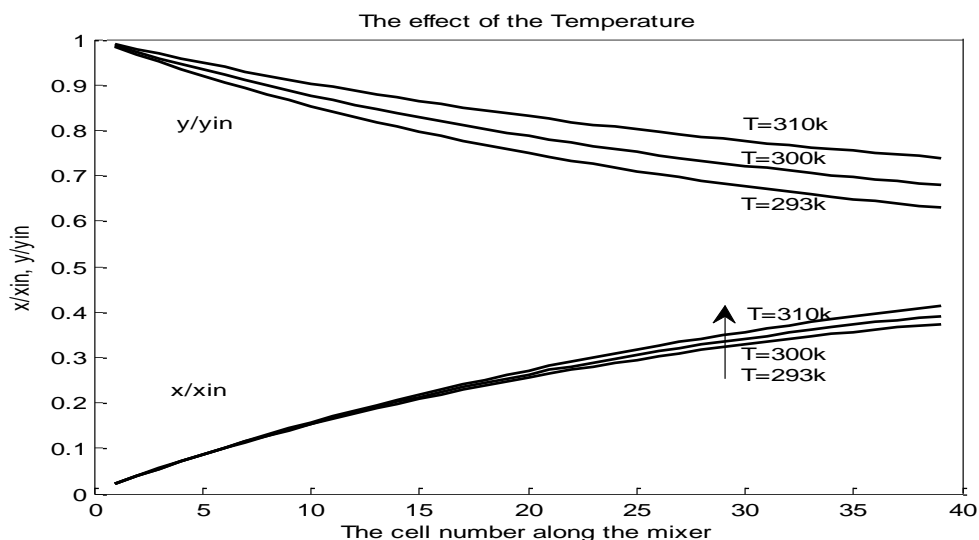


Figure 9: The effect of the temperature on the ozone concentration profile

4.6 THE EFFECT OF THE BACK FLOW RATIO (B) IN THE LIQUID PHASE ON THE OZONE MASS TRANSFER

The back flow ratio (B) can be defined as the fraction of the inlet main liquid flow to each cell that returned back from the upper stage to the lower adjacent stage. The back mixing in

the liquid phase is stronger due to the division of the fluid into several streams in opposite direction to the main flow in order to produce a homogeneous mixture.

Back mixing is characterised by two parameters: number of stages and the Peclet number and is estimated by the following equation: $B = \frac{N_{BFCM}}{Pe_L} - 0.5$. In the steady state BFCM, a value of 0.33 has been assigned to the back flow ratio (B) as it has been reported in the study of Tizaoui and Zhang, [1].

Figure 10 presents the effect of the backmixing in the liquid phase on the ozone gas and liquid concentrations along the static mixer. As the back flow ratio increases from 0.02 to 5, the liquid ozone concentration at the entrance of the static mixer (x/x_{in}^*) has increased from 0.03 to 0.12 while the ozone liquid concentration at the top of the static mixer remains almost the same.

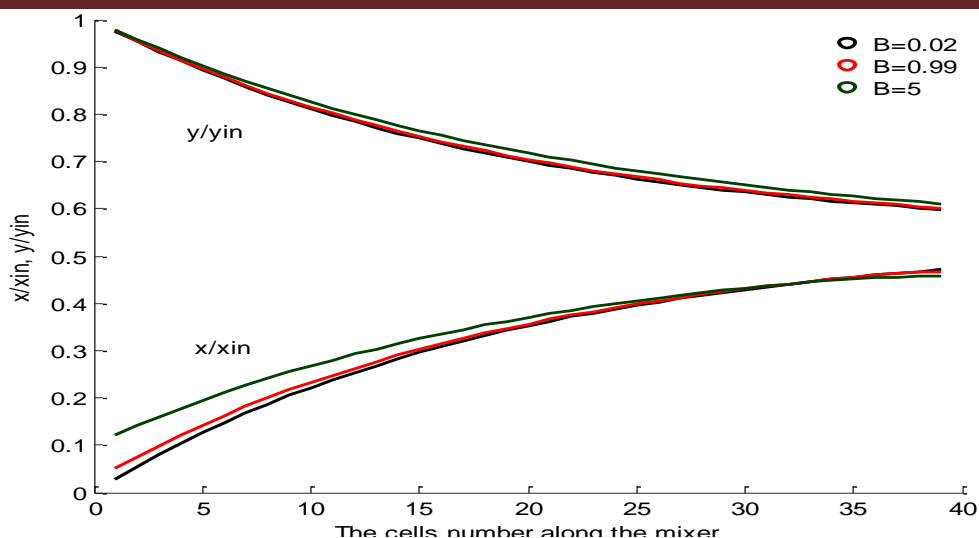


Figure 10: The impact of the back flow ratio (B) on the ozone concentration profile

The ozone concentration in the gas phase (y/y_{in}) has slightly increased along the whole height of the static mixer and this is maybe because of the backmixing in the gas phase was assumed to be negligible due to the high buoyancy of the gas phase. In contrast, the ozone concentration in the liquid phase (x/x_{in}^*) has only increased at the bottom of the mixer, but this increase in the concentration is becoming less noticeable as the liquid passes through the bottom of the static mixer. However, at the top of the static mixer, the liquid concentration

has remained the same for all three values of B. This can be explained by the fact that the liquid flow approaches plug flow conditions as it flows toward the top of the static mixer. As a result, the degree of back mixing decreases to a negligible value at the top of the mixer and therefore there is no change in the liquid ozone concentration at the top of the static mixer. In

a study conducted by Munter [2], it was found that at B=500, the decolorization degree spasmodically increased from zero to around 78%.

5.0 CONCLUSIONS

The steady state BFCM has predicted the gas and liquid ozone concentration profile across the height of the Kenics static mixer. The equations of the model have been numerically solved and transformed into the form of matrices and then implemented in a Matlab software. The impact of the main characteristic parameters of the steady state BFCM on ozone concentration profile in the gas and liquid phases along the height of the Kenics static mixer were analyzed using the Matlab software. These parameters are:

- The back flow ratio in the liquid phase
- The length of the Kenics static mixer
- Gas and liquid flow rates
- Volumetric liquid mass transfer coefficient
- Temperature

The effect of the liquid flow rate on the ozone concentration profile in the gas and the liquid phase and the ozone mass transfer efficiency of the mixer have been studied. It was found that the higher the liquid flow rates, the lower the ozone liquid concentration. Regarding the mass transfer efficiency, it was found that as the liquid flow rate increased it resulted in lower gas/liquid ratio, which increased the ozone mass transfer efficiency to around 94%. The later results proved the fact that the static mixers are more efficient at low gas/liquid ratio. Thus, static mixers can be successfully used for water ozonation.

The backmixing ratio has relatively little impact on the ozone liquid concentration. However, this impact reduces to a negligible value as the liquid flows toward the top of the mixer. Moreover, better mass transfer efficiency was obtained at higher lengths of static mixer but this will also result in higher capital cost and therefore a trade off is required.

6.0 FURTHER WORK

The steady state BFCM should be further developed and expanded in order account for the chemical reactions, especially the bromate formation.

The steady state BFCM should be further developed to account for the following parameters:

- The backmixing in the gas phase should be considered in order to study its influence on the hydrodynamic performance of the Kenics static mixer, especially in the cases where the gas phase largely deviates from the plug flow regimes.
- Variable back flow ratio in the liquid phase along the height of the static mixer should be included in the model. Since there is larger degree of mixing taking place at the inlet of the mixer than the outlet of the mixer, variable back flow ratio should be included in developing the BFCM, especially for the tall static mixers
- Variable cell volume along the height of the static mixer should be considered in developing the model and this very useful when modelling static mixers with multiple cells of variable dimensions.
- The models should be modified and expanded to account for variable mass transfer coefficient and cross sectional area along the Kenics static mixer.

REFERENCES:

- [1] Tizaoui, C., Zhang, Y. (2010), '**The modelling of ozone mass transfer in static mixers using Back Flow Cell Model**', Chemical Engineering Journal.
- [2] Munter, R. (2004) '**Mathematical modelling and simulation of ozonation process in a downstream static mixer with sieve plates**', Ozone Science & Engineering, 26 pp 227 – 236.
- [3] Heyouni, A, Roustan, M, Do-Quang, Z. (2002) '**Hydrodynamics and mass transfer in gas-liquid flow through static mixers**', Chemical Engineering Science , 57 , pp 3325 – 3333.
- [4] Roth, J. A., Sullivan, D. E. (1981) '**Solubility of ozone in water**', Ind. Eng. Chem. Fundam. 20 pp 137 – 140.
- [5] El-Din, M. G., Smith, D. W. (2001b) '**ozone mass transfer in water treatment: hydrodynamics and mass transfer modelling of ozone bubble columns**', Water Sci. Tech, 1, pp 123 – 130.
- [6] Masschelein, W. J. (2000) '**Fundamental properties of ozone in relation to water sanitation and environmental applications, in: I.O. Association (Ed.), Fundamental and Engineering concepts for ozone reactor design**, International ozone Association, Toulouse, France', pp 1 – 30.
- [7] Beers, K. J. (2001) **Numerical methods for Chemical Engineering: Application in Matlab**. Cambridge: Cambridge University Press.
- [8] Inashaie, S., Uhlig F., Affane C. (2001) **Numerical Techniques for Chemical and Biological Engineers Using Matlab: A Simple Bifurcation Approach**. New Yor: Springer.
- [9] Baawain, M. S., El-Din, M. G., Clarke., Katie and Smith, Daniel W. (2007) '**Impinging-Jet Ozone Bubble Column Modeling: Hydrodynamics, Gas Hold-up, Bubble Characteristics, and Ozone Mass Transfer**', Ozone: Science & Engineering, 29: 4, 245 — 259
- [10] Sanchez, C., Couvert, A., Laplanche, A., Renner, C. (2007) '**Hydrodynamic and mass transfer in a new co-current two-phase flow gas-liquid contactor**', Chemical Engineering Journal, 131, pp 49–58.
- [11] El-Din, M. G., Smith, D. W. (2001a) '**Development of Transient Back Flow Cell Model (BFCM) for Bubble Columns**', Ozone: Science & Engineering, 23, pp 313 – 326.

[12] Craik., Stephen. A., Finch., Gordon., Leparc., (2002) 'The effect of ozone gas-liquid contacting conditions in a static mixer on microorganism reduction', Ozone: Science & Engineering, 24, pp 91-103

8.0 APPENDICES

APPENDIX I - THE STEADY STATE BACK FLOW CELL MODEL

```
function[x,y,xs,u,s,d] = BFCM(N,V,L,G,T,PH,Pt,Kl,B,xin,yin)
```

```
D = 1.76*10^-9;
```

```
%D, ozone diffusivity coefficient
```

```
Kd = 5.43*10^3 * exp(-4964/T)
```

```
%Kd, pseudo first order ozone decay rate constant
```

```
Kl=0.1
```

```
%Kl, Volumetric liquid side mass transfer coefficient
```

```
Ha =sqrt((D*Kd)/Kl^2)
```

```
% Ha, Hatta number
```

```
if (Ha<1)
```

```
%D, ozone diffusivity coefficient
```

```
% Call Function[x,y,xs,u,s] =
```

```
BFCM(39,0.0054,0.03,0.0067,293.15,7,980,0.1,0.33,0,0.0640)
```

```
%INPUT
```

```
% N,cell number , % V, liquid cell volume
```

```
% L, liquid flow rate % G, Gas flow rate
```

```
% T, Temperature = 20 C = 293.15 K
```

```
% PH, acidity of water=7 , % Pt, Total pressure = 2 atm
```

```
% Kl. volumetric liquid mass transfer coefficient= 0.1 s-1
```

```
% B, back flow ratio = 0.33
```

```
% xin, inlet ozone liquid mole fraction
```

```
% yin, inlet ozone gas mole fraction
```

```
% OUTPOT
```

```
% x,ozone mole fraction in the liquid through the column
```

```
% y, mole fraction of zone in the gas through the column
```

```
% xs, equilibrium liquid mole fraction
```

```
% u, ratio = y/yin
```

```
% s, ratio = x/xsin where Xsin,is the inlet equilibrium mole fraction=yin/m
```

```
Kd = 5.43*10^3 * exp(-4964/T)
```

```
% Kd is the reaction rate constant
```

```
% d = 1.74*10^-9;
```

```
% Kw=4.667*10^-4;
```

```
% K=2*10^-3;
```

```
% Ha =sqrt((d*Kw)/K^2)
```

```
% if (Ha<1)
```

```
%Kd = 0.028
```

```
H = (3.84*10^7)*((10^(PH-14))^0.035) * exp(-2428/T)
```

```
% H is the henry constant
```

```
m = H/Pt
```

```
a0 = 1+B; a1 = 1+(2*B)+((Kl+Kd)*(V/L)); a2 = B; a3 =(Kl*V)/L; a4 = (Kl*V)/G;
```

```

LM = zeros(N,N);
LM = LM + diag(-a1*ones(N,1),0) + diag(a2*ones(N-1,1),1) + diag(a0*ones(N-1,1),-1);
LM(1,1)= a2-a1; LM(N,N)= a2-a1;
LB = zeros(N,1);LB(1,1)= -xin;
GM = zeros(N,N);
GM = GM + diag(-1*ones(N,1),0) + diag(1*ones(N-1,1),-1);
GB = zeros(N,1);GB(1,1)=(-yin);
C = GB -(a4*inv(LM)*LB);
A = GM -((a3*a4/m)*inv(LM))-((a4/m)*eye(N,N));
y = inv(A)* C;
x = (inv(LM)*LB)-((a3/m)*inv(LM)*inv(A)*C);
xs =(1/m)*inv(A)*C;
relrem = (y(N)-y(1))/y(N)
%relrem is ozone transfer percentage
u = y/yin;
xsin = yin/m;
s = x/xsin;
f=1:1:39
figure(1)
plot(f,u,'k',f,s,'r')
xlabel('the mixer length, z'), ylabel('x/xin, y/yin')
disp('  x    y    xs    u    s ');
disp([x,y,xs,u,s,[1:length(x)]]')
end
end

```

APPENDIX II - THE EFFECT OF THE MAIN PARAMETERS OF THE STEADY STATE BFCM

```

clear all
close all
clc
for i=1:6
if i==1
for Kl=[ 0.09 0.15 0.2 0.3];
N = 39;V =0.00553;L = 0.03;G = 0.00667;T = 293.15;PH=3;Pt = 980;B = 0.33;xin = 0;yin = 0.064;
Kd = 5.43*10^3 * exp(-4964/T);H = (3.84*10^7)*((10^(PH-14))^0.035) * exp(-2428/T);
m = H/Pt;a0 = 1+B; a1 = 1+(2*B)+((Kl+Kd)*(V/L)); a2 = B; a3 =(Kl*V)/L; a4 = (Kl*V)/G;
LM = zeros(N,N);LM = LM + diag(-a1*ones(N,1),0)+ diag(a2*ones(N-1,1),1) + diag(a0*ones(N-1,1),-1);
LM(1,1)= a2-a1; LM(N,N)= a2-a1;LB = zeros(N,1);LB(1,1)= -xin;
GM = zeros(N,N);GM = GM + diag(-1*ones(N,1),0) + diag(1*ones(N-1,1),-1);GB = zeros(N,1);GB(1,1)=(-yin);
C = GB -(a4*inv(LM)*LB);A = GM -((a3*a4/m)*inv(LM))-((a4/m)*eye(N,N));
y = inv(A)* C;x = (inv(LM)*LB)-((a3/m)*inv(LM)*inv(A)*C);
xs =(1/m)*inv(A)*C;u = y/yin;xsin = yin/m;s = x/xsin;
f=1:1:39,figure(i),hold on plot(f,u,'k',f,s,'r')
xlabel('The cell number'), ylabel('x/xin, y/yin'),title('The effect of mass transfer coefficient')
end
end
if i==2

```

```

for G=[0.0033 0.0067 0.0133 0.0167 ];
N = 39;V =0.0054;L = 0.03;T = 290;PH=6;Pt = 880;Kl= 0.1;B = 0.33;xin = 0;yin = 0.064,

Kd = 5.43*10^3 * exp(-4964/T);H = (3.84*10^7)*((10^(PH-14))^0.035) * exp(-2428/T);
m = H/Pt;a0 = 1+B; a1 = 1+(2*B)+((Kl+Kd)*(V/L)); a2 = B; a3 =(Kl*V)/L; a4 = (Kl*V)/G;

LM = zeros(N,N);LM = LM + diag(-a1*ones(N,1),0)+ diag(a2*ones(N-1,1),1) +
diag(a0*ones(N-1,1),-1);
LM(1,1)= a2-a1; LM(N,N)= a2-a1;LB = zeros(N,1);LB(1,1)= -xin;
GM = zeros(N,N);GM = GM + diag(-1*ones(N,1),0) + diag(1*ones(N-1,1),-1);GB =
zeros(N,1);GB(1,1)=(-yin);
C = GB -(a4*inv(LM)*LB);A = GM -((a3*a4/m)*inv(LM))-((a4/m)*eye(N,N));
y = inv(A)* C;x = (inv(LM)*LB)-((a3/m)*inv(LM)*inv(A)*C);
xs =(1/m)*inv(A)*C;u = y/yin;xsin = yin/m;s = x/xsin;
f=1:1:39,figure(i),hold on,plot(f,u,'k',f,s,'r')
xlabel('The cell number'), ylabel('x/xin, y/yin'),title('The effect of gas flow rate')
end
end
if i==3
for B=[ 0.02 0.99 5]
N = 39;V =0.0054;L = 0.03;G = 0.00667;T = 293.15;PH=3;Pt = 880;Kl= 0.1;xin = 0;yin =
0.064
Kd = 5.43*10^3 * exp(-4964/T);H = (3.84*10^7)*((10^(PH-14))^0.035) * exp(-2428/T);
m = H/Pt;a0 = 1+B; a1 = 1+(2*B)+((Kl+Kd)*(V/L)); a2 = B; a3 =(Kl*V)/L; a4 = (Kl*V)/G;
LM = zeros(N,N);LM = LM + diag(-a1*ones(N,1),0)+ diag(a2*ones(N-1,1),1) +
diag(a0*ones(N-1,1),-1);
LM(1,1)= a2-a1; LM(N,N)= a2-a1;LB = zeros(N,1);LB(1,1)= -xin;
GM = zeros(N,N);GM = GM + diag(-1*ones(N,1),0) + diag(1*ones(N-1,1),-1);GB =
zeros(N,1);GB(1,1)=(-yin);
C = GB -(a4*inv(LM)*LB);A = GM -((a3*a4/m)*inv(LM))-((a4/m)*eye(N,N));
y = inv(A)* C;x = (inv(LM)*LB)-((a3/m)*inv(LM)*inv(A)*C);
xs =(1/m)*inv(A)*C;u = y/yin;xsin = yin/m;s = x/xsin;
f=1:1:39,figure(i),hold on,plot(f,u,'k',f,s,'r')
xlabel('The cell number'), ylabel('x/xin, y/yin'),title('The effect of Backmixing ratio(B)')
end
end
if i==4
for V=[0.0054 0.0147 0.0206 ]
N = 39;L = 0.03;G = 0.00667;T = 293.15;PH=3;Pt = 880;Kl= 0.1;B = 0.33;xin = 0;yin =
0.064
Kd = 5.43*10^3 * exp(-4964/T);H = (3.84*10^7)*((10^(PH-14))^0.035) * exp(-2428/T);
m = H/Pt;a0 = 1+B; a1 = 1+(2*B)+((Kl+Kd)*(V/L)); a2 = B; a3 =(Kl*V)/L; a4 = (Kl*V)/G;
LM = zeros(N,N);LM = LM + diag(-a1*ones(N,1),0)+ diag(a2*ones(N-1,1),1) +
diag(a0*ones(N-1,1),-1);

LM(1,1)= a2-a1; LM(N,N)= a2-a1;LB = zeros(N,1);LB(1,1)= -xin;
GM = zeros(N,N);GM = GM + diag(-1*ones(N,1),0) + diag(1*ones(N-1,1),-1);GB =
zeros(N,1);GB(1,1)=(-yin);
C = GB -(a4*inv(LM)*LB);A = GM -((a3*a4/m)*inv(LM))-((a4/m)*eye(N,N));
y = inv(A)* C;x = (inv(LM)*LB)-((a3/m)*inv(LM)*inv(A)*C);

```

```

xs=(1/m)*inv(A)*C;u = y/yin;xsin = yin/m;s = x/xsin;
f=1:1:39,figure(i),hold on,plot(f,u,'k',f,s,'r')

xlabel('The cell number'), ylabel('x/xin, y/yin'),title('The effect of the length of the mixer')
end
end
if i==5
for L=[0.005 0.0167 0.033 0.0667 ];
Kl=0.1;N = 39;V =0.0054;G = 0.00667;T = 293.15;PH=3;Pt = 880;B = 0.33;xin = 0;yin =
0.064;
Kd = 5.43*10^3 * exp(-4964/T);H = (3.84*10^7)*((10^(PH-14))^0.035) * exp(-2428/T);
m = H/Pt;a0 = 1+B; a1 = 1+(2*B)+((Kl+Kd)*(V/L)); a2 = B; a3 =(Kl*V)/L; a4 =(Kl*V)/G;
LM = zeros(N,N);LM = LM + diag(-a1*ones(N,1),0)+ diag(a2*ones(N-1,1),1) +
diag(a0*ones(N-1,1),-1);
LM(1,1)= a2-a1; LM(N,N)= a2-a1;LB = zeros(N,1);LB(1,1)= -xin;
GM = zeros(N,N);GM = GM + diag(-1*ones(N,1),0) + diag(1*ones(N-1,1),-1);GB =
zeros(N,1);GB(1,1)=(-yin);
C = GB -(a4*inv(LM)*LB);A = GM -((a3*a4/m)*inv(LM))-((a4/m)*eye(N,N));
y = inv(A)* C;x = (inv(LM)*LB)-((a3/m)*inv(LM)*inv(A)*C);
xs=(1/m)*inv(A)*C;u = y/yin;xsin = yin/m;s = x/xsin;
f=1:1:39,figure(i),hold on,plot(f,u,'k',f,s,'r')
xlabel('the mixer length, z'), ylabel('x/xin, y/yin'),title('The effect of liquid flow rate')
end
end
if i==6
for T=[293.15 300 310]
N = 39;V =0.0054;L = 0.03;G = 0.00667;PH=3;Pt = 880;Kl= 0.1;B = 0.33;xin = 0;yin =
0.064
Kd = 5.43*10^3 * exp(-4964/T);H = (3.84*10^7)*((10^(PH-14))^0.035) * exp(-2428/T);
m = H/Pt;a0 = 1+B; a1 = 1+(2*B)+((Kl+Kd)*(V/L)); a2 = B; a3 =(Kl*V)/L; a4 =
(Kl*V)/G;
LM = zeros(N,N);LM = LM + diag(-a1*ones(N,1),0)+ diag(a2*ones(N-1,1),1) +
diag(a0*ones(N-1,1),-1);
LM(1,1)= a2-a1; LM(N,N)= a2-a1;LB = zeros(N,1);LB(1,1)= -xin;
GM = zeros(N,N);GM = GM + diag(-1*ones(N,1),0) + diag(1*ones(N-1,1),-1);GB =
zeros(N,1);GB(1,1)=(-yin);
C = GB -(a4*inv(LM)*LB);A = GM -((a3*a4/m)*inv(LM))-((a4/m)*eye(N,N));

y = inv(A)* C;x = (inv(LM)*LB)-((a3/m)*inv(LM)*inv(A)*C);
xs=(1/m)*inv(A)*C;u = y/yin;xsin = yin/m;s = x/xsin;
f=1:1:39,figure(i),hold on ,plot(f,u,'k',f,s,'r'),
xlabel('The cell number'), ylabel('x/xin, y/yin'), title('The effect of the Temperature')
end
end
end

```